Solid-State Electronics 197 (2022) 108439

Contents lists available at ScienceDirect

Solid State Electronics

journal homepage: www.elsevier.com/locate/sse

Massively parallel FDTD full-band Monte Carlo simulations of electromagnetic THz pulses in p-doped silicon at cryogenic temperatures

C. Jungemann [a,*], F. Meng [b], M.D. Thomson [b], H.G. Roskos [b]

[a] Chair of Electromagnetic Theory, RWTH Aachen University, Aachen 52056, Germany
[b] Physikalisches Institut, Goethe-Universität Frankfurt, Frankfurt am Main 60438, Germany

ARTICLE INFO

Keywords:
FDTD
Monte Carlo
Electromagnetic waves
Higher harmonics

ABSTRACT

In semiconductor samples with a low density of free charge carriers the current response to an intense electromagnetic pulse is weak and can be treated as a perturbation in the finite-difference-time-domain calculation of the electromagnetic field. Up to first order the electric field that drives the particles does not depend on their density and the particles can be simulated independently. This opens the door for massively parallel Monte Carlo simulations that can be processed efficiently on a computer cluster and a large number of particles can be simulated resulting in a very low noise level. By this full-band Monte Carlo finite-difference-time-domain approach the generation of higher harmonics in p-doped silicon at cryogenic temperatures is investigated. It is found that the higher harmonics are mostly due to the warped valence bands, which are discretized on adaptive unstructured tetrahedral grids in the k-space to avoid numerical artifacts.

1. Introduction

Intense electromagnetic THz pulses lead to a nonlinear response of the particle gas in semiconductor materials and result in the generation of higher harmonics [1]. These higher harmonics, which are due to the nonparabolic band structure and energy-dependent scattering, can be used to probe properties of the semiconductors [2]. Here we theoretically investigate experiments where an intense THz pulse passes through a weakly p-doped silicon layer (thickness 275μm) where the beam is normal to the [001] surface of the layer and the linearly polarized electric field is aligned with the [100] direction. The sample is kept at a temperature of 10K and the hole density is much lower than the acceptor concentration of $5\times10^{16}\mathrm{cm}^{-3}$ due to impurity freeze-out. While the pump field dependence indicates that additional carriers are generated during the pulse (attributed to impact ionization [3]), here we assume a constant total population of holes, which still captures the main aspects of the harmonic generation. In measurements the intensity of the 3rd harmonic is many orders of magnitude lower than the fundamental one confirming that the hole density is indeed very low.

2. Simulation Model

Because of the rather large diameter of the beam and that the measured harmonics are dominated by the high intensity at the beam center the electromagnetic field can be approximated for the simulation by a linearly polarized plane TEM wave. The wave propagates into the positive z direction and the electric and magnetic fields are aligned with the x and y directions, respectively. In this case Maxwell's equations reduce to [4]

$$-\frac{\partial H_y}{\partial z}=J_x+\varepsilon_r\varepsilon_0\frac{\partial E_x}{\partial t}, \tag{1}$$

$$\frac{\partial E_x}{\partial z}=-\mu_0\frac{\partial H_y}{\partial t}. \tag{2}$$

H_y is the y component of the magnetic field strength, E_x the x component of the electric field strength, J_x the x component of the current density, ε_0 the electric field constant of the vacuum, ε_r the relative permittivity, and μ_0 the magnetic field constant of the vacuum. A longitudinal electric field which could occur due to an inhomogeneous distribution of the holes in the silicon layer is neglected, because the net space charge density of the ionized acceptors and holes is very low [5].

The hole current density in the silicon layer caused by the transverse electric field is proportional to the low hole density and it can be treated as a perturbation in Maxwell's equations. It is multiplied with the dimensionless parameter λ [6]

* Corresponding author.
E-mail address: cj@ithe.rwth-aachen.de (C. Jungemann).

https://doi.org/10.1016/j.sse.2022.108439
Received 21 June 2022; Received in revised form 2 August 2022; Accepted 18 August 2022
Available online 24 August 2022

$$-\frac{\partial H_y}{\partial z} = \lambda J_x + \varepsilon_r \varepsilon_0 \frac{\partial E_x}{\partial t}, \tag{3}$$

$$\frac{\partial E_x}{\partial z} = -\mu_0 \frac{\partial H_y}{\partial t} \tag{4}$$

and the fields are expanded into a power series w.r.t. λ

$$H_y = H_y^{(0)} + \lambda H_y^{(1)} + \cdots, \tag{5}$$

$$E_x = E_x^{(0)} + \lambda E_x^{(1)} + \cdots. \tag{6}$$

The zero order fields are the solutions of

$$-\frac{\partial H_y^{(0)}}{\partial z} = \varepsilon_r \varepsilon_0 \frac{\partial E_x^{(0)}}{\partial t}, \tag{7}$$

$$\frac{\partial E_x^{(0)}}{\partial z} = -\mu_0 \frac{\partial H_y^{(0)}}{\partial t}, \tag{8}$$

where the current density does not occur, because it is multiplied by λ. The first order fields satisfy

$$-\frac{\partial H_y^{(1)}}{\partial z} = J_x^{(0)} + \varepsilon_r \varepsilon_0 \frac{\partial E_x^{(1)}}{\partial t}, \tag{9}$$

$$\frac{\partial E_x^{(1)}}{\partial z} = -\mu_0 \frac{\partial H_y^{(1)}}{\partial t}. \tag{10}$$

where $J_x^{(0)}$ appears, which is calculated based on $E_x^{(0)}$ which does not depend on $J_x^{(0)}$.

This makes it possible to decouple the pump-pulse propagation and the response of the hole gas, which greatly reduces the computational cost of the simulations. The electromagnetic field is calculated by the finite-difference-time-domain (FDTD) method [7,5] and the hole current density by Monte Carlo (MC) simulations [8]. The algorithm consists of three steps:

1. The electromagnetic pulse is simulated for a vanishing hole density by a 1D FDTD solver with perfectly absorbing boundaries and the electric field in the silicon layer is recorded as a function of location and time. This yields $E_x^{(0)}(z,t)$.
2. For this electric field transient bulk simulations are performed by a full-band MC code [9], where the movement of the holes in z direction is neglected due to the large wave length and the particles can be simulated independently w.r.t. their position in the real space. Jobs are started in parallel for all the boxes of the real space grid in the silicon region. This yields $J_x^{(0)}(z,t)$.[1]
3. A FDTD simulation with the current density obtained in the second step and a zero source field is performed, where the electric field at the fundamental frequency caused by the current density is much smaller than the one due to the THz source, and a first order perturbation approach suffices. This yields $E_x^{(1)}(z,t)$.

The transmitted electric field is obtained with $\lambda = 1$ and $|E_x^{(0)}| \gg |E_x^{(1)}| \gg |E_x^{(2)}|$ by $E_x^{(0)} + E_x^{(1)}$. Its spectrum is given by the absolute square of its Fourier transform and does not depend on the position in the vacuum.

In the case of holes the warped valence bands have a strong impact on the generation of higher harmonics and a full-band MC simulation is required, which is described in detail in Ref. [9]. The band structure is calculated by the nonlocal empirical pseudopotential method including spin–orbit coupling [10]. For each individual valence band an unstructured tetrahedral mesh is generated that satisfies certain quality criteria [11,9]. The energy is linearly interpolated within a tetrahedron and continuous when moving to an adjacent tetrahedron. The mesh fills the complete irreducible wedge of the first Brillouin zone and has the necessary symmetries on the surface of the wedge to ensure a continuous energy band when changing from one Brillouin zone into the next [9].

The interpolated dispersion relations of the valence bands have to be sufficiently smooth to avoid spurious generation of higher harmonics. Since the interpolation is only piecewise linear, a fine grid is required. The grid resolution is controlled by a relative error criterion for the energy difference between the interpolated energy and the energy calculated directly by the pseudopotential method, where the difference must be less than 2% of the energy or less than 50μeV, whatever limit is larger. This results in a very fine grid close to the Γ point (Fig. 1). This high resolution at low hole energies is necessary to avoid problems at low temperatures. In addition, the grid has to satisfy two further criteria. The maximal length of an edge of a tetrahedron is limited and the volume to surface ratio must be sufficiently large to avoid flat tetrahedra. The number of k-grid points and tetrahedra in the irreducible wedge is given in Table 1. We have checked by simulations with finer grids that the k-space mesh has a negligible impact on the results.

3. Results

A spacing of 0.25μm and a time step of 0.417fs is used to resolve the higher harmonics in space and time. The number of boxes in the silicon layer is 1100 and in each box 125,000 particles are simulated resulting in a total of 1.375×10^8 particles. The CPU time for a single box is about 8 h and the total CPU time about a year. The CPU time of the independent MC simulations is large compared to the FDTD simulations which take only seconds, and the MC jobs are processed by a batch system to make the best use of the computer cluster. The wall clock time for the complete simulation is less than a day.

The electric field of the source pulse is given by a sinusoidal carrier wave with a frequency of 1.29THz and a Gaussian envelope function (Fig. 2). A fraction of the pulse is reflected at both interfaces between the sample and vacuum leading to a partially standing wave in the vacuum at the source side and in the sample. The maximum value of the magnitude of the electric field over time is shown in Fig. 3, and the maximal electric field strongly varies in the sample. This result clearly shows that the reflection of the wave at both interfaces has a strong impact on the amplitude and phase of the spectral components as a

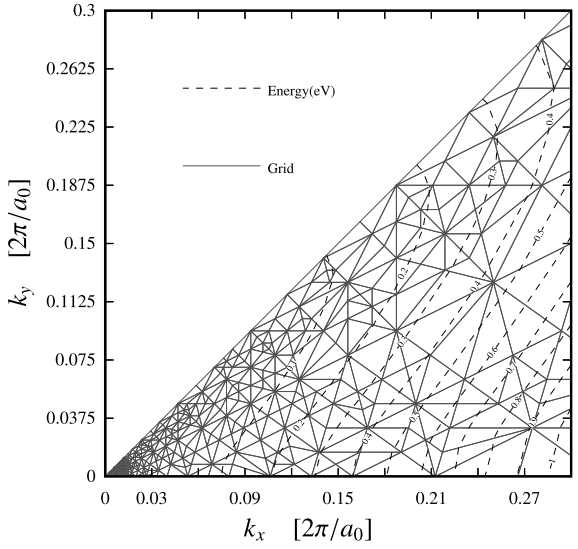

Fig. 1. K-space grid of the heavy-hole band of silicon for $k_z = 0$ near the Γ point [9]. a_0 is the lattice constant of silicon.

[1] In the calculation of the hole velocity the magnetic field is neglected, because the Lorentz force is less than a percent of the electric force due to the low velocity of the holes compared to the speed of light in silicon.

Table 1
Number of grid points and tetrahedra in the irreducible wedge of relaxed silicon for the heavy-hole (hh), light-hole (lh) and split-off (so) bands.

Band	k-points	tetrahedra
hh	3082	13111
lh	2209	9354
so	1284	5226

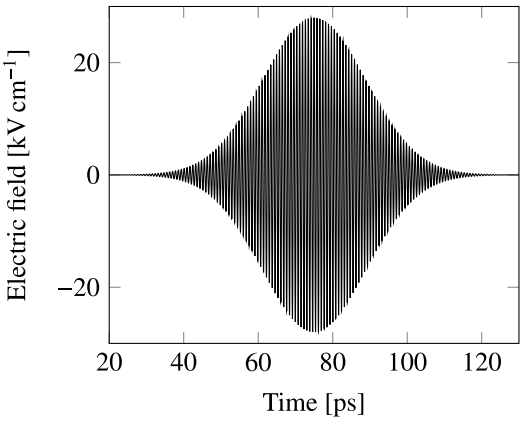

Fig. 2. Electric field of the THz pulse generated by the source for an amplitude of 28 kV cm^{-1}.

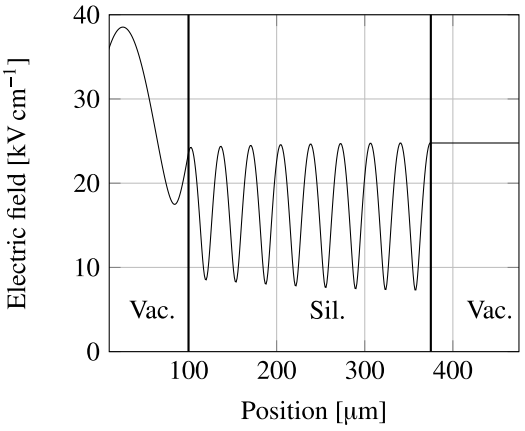

Fig. 3. Maximum of the pump-pulse electric field over time versus location for a source amplitude of 28kV cm^{-1}.

function of position and that a transient device simulation of the electromagnetic field is necessary.

The higher harmonics are due to the current response of the holes. Since the zero order electromagnetic field is strongly inhomogeneous in the silicon layer (Fig. 3), the current response has to be calculated as a function of space and time as well. In Fig. 4 the envelope functions of the velocity response and electric field at the first minimim of the maximal electric field inside the silicon layer ($z = 120\mu m$) and at the last maximum ($z = 341\mu m$) are shown. At the minimum the electric field and the velocity show a small echo after 100ps. Due to the larger electric field, the velocity response at $z = 341\mu m$ is much larger and more nonlinear with stronger harmonics. The maximum of the electric field is shifted by about 7ps. This shift is smaller for the hole velocity, because in the case of the larger electric field the hole gas becomes hot and the velocity is reduced by the increased scattering. The asymmetry of the velocity response is due to the large energy relaxation time at this low lattice temperature and the mean energy is larger during the falling edge than during the rising edge. This complex spatiotemporal behavior has

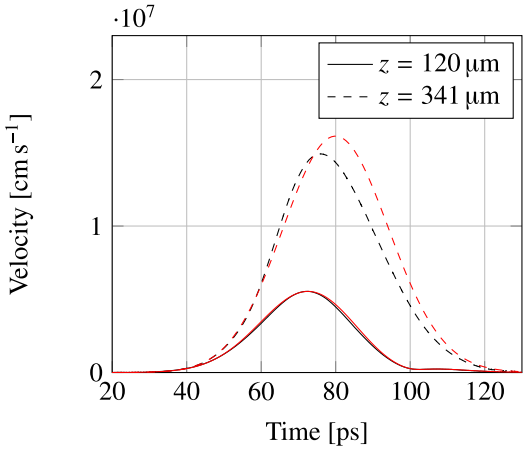

Fig. 4. Envelope functions of the average hole velocity (black lines) and electric field times a mobility of 6.5 × 10^{5}cm^2 V^{-1} s^{-1} (red lines) for two different positons in the silicon layer.

to be taken into account, when the transmitted electromagnetic field is calculated. In addition, this ensures that all interference effects are included in the wave calculation.

In the experiments the intensity of the transmitted electric field is measured as a function of the frequency. The intensity is the absolute square of the Fourier transform of the transmitted electric field and at odd multiples of the fundamental frequency additional peaks occur. Since the intensity of the fundamental frequency is many orders of magnitude larger than the higher harmonics, filters have to be used to suppress it in the measurement of the higher harmonics. This makes it difficult to determine the absolute magnitude of the higher harmonics and the main result is the ratio of the 3rd and 5th harmonic. In the first order perturbation calculations the higher harmonics are proportional to the square of the hole current density and thus proportional to the square of the hole density, which cancels when the ratio of the harmonics is calculated. Therefore, the absolute value of the hole density does not matter as long as its value is orders of magnitude smaller than the acceptor concentration and a first order perturbation approximation holds. In Fig. 5 the simulated intensity is shown and the ratio of the 3rd and 5th harmonic is 313. The resultant noise is very low due to the large number of simulated particles and their independent simulation, and even the 9th harmonic is clearly visible in Fig. 5.

In Fig. 6 the result of a transient bulk MC simulation is shown, where the electric field is given by the source field. The intensity is calculated based on the time-dependent velocity. The resultant ratio of the 3rd and 5th harmonic is 15.4 and much smaller than in the case of the FDTD MC

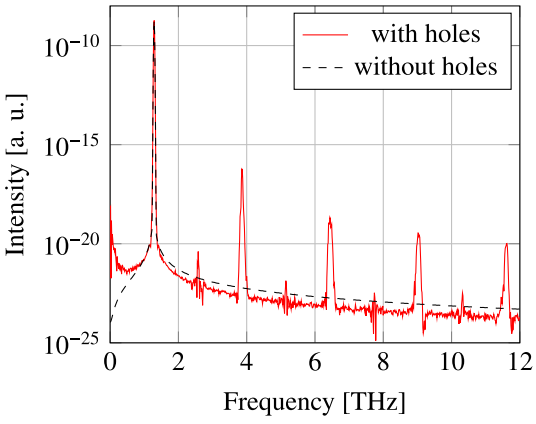

Fig. 5. Intensity of the transmitted electric field for a source amplitude of 28kV cm^{-1} and frequency of 1.29THz.

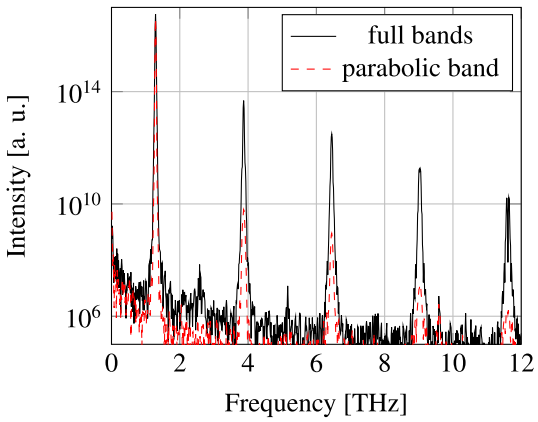

Fig. 6. Intensity of the bulk velocity for an amplitude of 24kV cm^{-1} and frequency of 1.29THz for full bands and a parabolic band with a similar effective mass.

simulation, showing that a simple bulk MC simulation is not sufficient to quantitatively describe the generation of higher harmonics in the silicon layer and the full wave propagation has to be taken into account. Furthermore, results are shown for simulations with a parabolic band with a similar effective mass as the full bands. The higher harmonics are reduced by orders of magnitude showing that their generation is mostly due to the warped valance bands.

4. Conclusions

In the case of a weakly doped semiconductor sample the current response of the particle gas to an intense electromagnetic pulse can be treated as a perturbation, and the particles in the MC run can be simulated independently. This enables efficient parallelization on a computer cluster, because more than 99% of the wall clock time are spent for the MC simulations. Due to the large number of simulation particles that can be processed within hours of wall clock time and the noiseless electric field on which the MC simulations are based, the noise level of the transmitted electric field is very low.

At a lattice temperature of 10K the generation of higher harmonics is mostly due to the warped valence bands and to a lesser extend caused by the energy dependent scattering.

Declaration of Competing Interest

The authors declare that they have no known competing financial interests or personal relationships that could have appeared to influence the work reported in this paper.

Data availability

Data will be made available on request.

References

[1] Ghimire S, DiChiara AD, Sistrunk E, Agostini P, DiMauro LF, Reis DA. Observation of high-order harmonic generation in a bulk crystal. Nat Phys 2011;7(2):138–41. https://doi.org/10.1038/nphys1847. URL:https://doi.org/10.1038/nphys1847.

[2] Meng F, Walla F, ul Islam Q, Thomson MD, Kovalev S, Deinert J-C, et al., High-harmonic generation from weakly p-doped Si pumped with intense THz pulses. In: 2021 46th International Conference on Infrared, Millimeter and Terahertz Waves (IRMMW-THz), 2021, pp. 1–1. doi:10.1109/IRMMW-THz50926.2021.9567287.

[3] Meng F, Thomson MD, ul Islam Q, Klug B, Pashkin A, Schneider H, Roskos HG, Intracavity third-harmonic generation in Si:B pumped by intense terahertz pulses, Phys. Rev. B 102 (2020) 075205. doi:10.1103/PhysRevB.102.075205. URL: https://link.aps.org/doi/10.1103/PhysRevB.102.075205.

[4] Jackson JD, Classical Electrodynamics, 2nd Edition, John Wiley & Sons, New York, 1975.

[5] Willis KJ, Ayubi-Moak JS, Hagness SC, Knezevic I. Global modeling of carrier-field dynamics in semiconductors using EMC–FDTD. J Comput Electron 2009;8(2):153. https://doi.org/10.1007/s10825-009-0280-4.

[6] Bender CM, Orszag SA. Advanced mathematical methods for scientists and engineers I: asymptotic methods and perturbation theory. New York: Springer; 1999.

[7] Yee K. Numerical solution of initial boundary value problems involving Maxwell's equations in isotropic media. IEEE Trans Antennas Propag 1966;14(3):302–7. https://doi.org/10.1109/TAP.1966.1138693.

[8] Jacoboni C, Reggiani L. The Monte Carlo method for the solution of charge transport in semiconductors with applications to covalent materials. Rev Mod Phys 1983;55:645–705. https://doi.org/10.1103/RevModPhys.55.645.

[9] Jungemann C, Meinerzhagen B. Hierarchical Device Simulation: The Monte-Carlo Perspective, Computational Microelectronics. Wien, New York: Springer; 2003.

[10] Ungersboeck E, Dhar S, Karlowatz G, Sverdlov V, Kosina H, Selberherr S. The effect of general strain on the band structure and electron mobility of silicon. IEEE Trans Electron Devices 2007;54(9):2183–90. https://doi.org/10.1109/TED.2007.902880.

[11] Bude J, Smith RK. Phase-space simplex Monte Carlo for semiconductor transport. Semicond Sci Technol 1994;9(5S):840–3. https://doi.org/10.1088/0268-1242/9/5s/119.